Field Quality Measurements of LARP Nb_3Sn Magnet HQ02

J. DiMarco, G. Ambrosio, M. Buehler, G. Chlachidze, D. Orris, C. Sylvester, M.Tartaglia, G. Velev, M. Yu, A.V. Zlobin, A. Ghosh, J. Schmalzle, P. Wanderer, F. Borgnolutti, D. Cheng, D. Dietderich, H. Felice, A. Godeke, R. Hafalia, J. Joseph, J. Lizarazo, M. Marchevsky, S. O. Prestemon, G.L. Sabbi, A. Salehi, X. Wang, P. Ferracin, E. Todesco

***Abstract*— Large-aperture, high-field, Nb_3Sn quadrupoles are being developed by the US LHC accelerator research program (LARP) for the High luminosity upgrade of the Large Hadron Collider (HiLumi-LHC). The first 1 m long, 120 mm aperture prototype, HQ01, was assembled with various sets of coils and tested at LBNL and CERN. Based on these results, several design modifications have been introduced to improve the performance for HQ02, the latest model. From the field quality perspective, the most relevant improvements are a cored cable for reduction of eddy current effects, and more uniform coil components and fabrication processes. This paper reports on the magnetic measurements of HQ02 during recent testing at the Vertical Magnet Test Facility at Fermilab. Results of baseline measurements performed with a new multi-layer circuit board probe are compared with the earlier magnet. An analysis of probe and measurement system performance is also presented.**

***Index Terms*— Field quality, Magnetic Measurement, Superconducting accelerator magnets.**

I. Introduction

In preparation for the high luminosity upgrade of the Large Hadron Collider, the LHC Accelerator Research Program (LARP) is developing a new generation of large aperture high-field quadrupoles based on Nb_3Sn technology [1]. HQ02 is a 1-meter long, 120 mm diameter Nb_3Sn quadrupole made as part of development of quadrupoles with eventual aperture of 150 mm. Tests of the first series of HQ coils revealed the necessity for further optimization of the coil design and fabrication process. A new model (HQ02) has been fabricated with several modifications implemented. From the point of view of magnetic design, the performance of HQ02 should be accelerator quality – the cross–section has been optimized to limit harmonics and the cored cable should limit the eddy current effects. This paper reviews the magnetic measurements performed on HQ02 at Fermilab's Vertical Magnet Test Facility (VMTF) and discusses some results pertaining to magnet and measurement quality. Additional analysis of dynamic effects can be found at another paper to this conference [2].

Manuscript received July 16, 2013. This work was supported by the U.S. LHC Accelerator Research Program through US Department of Energy contracts DE-AC02-07CH11359, DE-AC02-98CH10886, DE-AC02-05CH11231, and DE-AC02-76SF00515. It was also supported by EU FP7 HiLumi LHC – Grant Agreement 284404.

J. DiMarco, G. Ambrosio, M. Buehler, G. Chlachidze, D. Orris, C. Sylvester, M.Tartaglia, G. Velev, M. Yu, A.V. Zlobin are with Fermi National Accelerator Laboratory, P.O. Box 500, Batavia, IL 60510, USA, (phone: 630-840-2672; fax: 630-840-8079; e-mail: dimarco@fnal.gov).

A. Ghosh, J. Schmalzle, P. Wanderer are with Brookhaven National Laboratory, Upton, NY, 11973-5000 USA.

F. Borgnolutti, D. Cheng, D. Dietderich, H. Felice, A. Godeke, R. Hafalia, J. Joseph, J. Lizarazo, M. Marchevsky, S. O. Prestemon, G.L. Sabbi, A. Salehi, X. Wang are with Lawrence Berkeley National Laboratory, Berkeley, CA 94720 USA.

P. Ferracin, E. Todesco are with the the European Organization for Nuclear Research, CERN CH-1211, Genève 23, Switzerland.

II. Magnet Design and Parameters

HQ02 has been designed to reach gradients above 200 T/m at 1.9 K in a 120 mm aperture. The first HQ used a 15.15 mm wide cable made with both RRP 54/61 and RRP 108/127 conductor in a 2-layer design. Coils for HQ02 by contrast have smaller width, 14.75 mm, and slightly smaller strand size (0.778 mm vs. 0.8 mm for HQ01) and are fabricated with (Ta doped) RRP 108/127 sub-element design conductor. The smaller cable prevented over-compaction and excessive strain during the reaction phase which had been observed in first generation models, leading to conductor damage and oversized coils in the first generation models. As a result, the new set of coils are more uniform and closer to the design size. However, they still do not constitute an identical set due to various design changes that were applied, most notably in the cable insulation and end parts. The HQ02 cable, in addition, has a 25 micron thick stainless steel core which extends over a width of 8 mm, biased toward the thick cable edge. This represents about 60% coverage of the available width. The cable thickness is 1.375 mm – less than the 1.437 mm of HQ01 – to help avoid over-compaction of the coil. A detailed overview of design features can be found in [3].

III. Magnetic Measurements

The magnetic field in the aperture of the quadrupole is expressed in terms of harmonic coefficients defined in a series expansion using the complex function formalism

$$B_y + iB_x = B_2 10^{-4} \sum_{n=1}^{\infty} (b_n + ia_n) \left(\frac{x+iy}{R_{ref}} \right)^{n-1} \qquad (1)$$

where B_x and B_y in (1) are the horizontal and vertical field components in the Cartesian coordinates, b_n and a_n are the $2n$-pole normal and skew harmonic coefficients at the reference radius R_{ref}= 40 mm [4]. The right-handed measurement coordinate system is defined with the z-axis at the center of the magnet aperture and pointing from return to lead end.

The magnetic measurements were performed using the standard acquisition system at VMTF [5] together with a new 10-layer Printed Circuit Board (PCB) probe, having both 100 mm long and 200 mm long windings on a single board [6]. The PCB probe and holder are shown in Fig. 1.

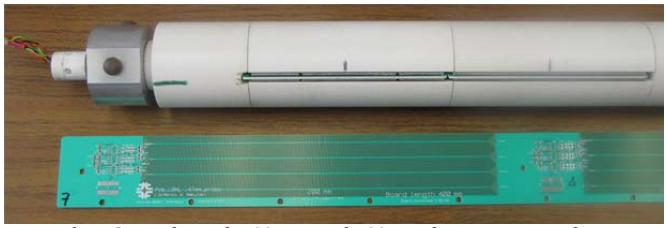

Fig.1. The PCB probe with 200-mm and 100-mm long, 47 mm in diameter probes (bottom) and PCB probe holder (top). Probe rotation speed is 1 Hz.

The windings include an analog bucked signal which achieved reduction of the main field by a factor of ~480/1100 for the 100 mm / 200 mm circuits respectively. The resolution of the probe for cold measurements can be estimated from Fig. 2 to be on the order of 0.002 units through the n=10 harmonic at the probe radius of 23.5 mm (this is effectively about 0.3 units through n=10 at the 40 mm radius) [7].

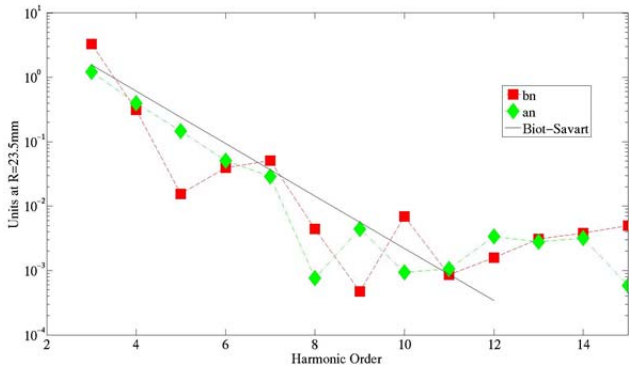

Fig.2. Probe resolution - estimated by comparing results during measurements at 1.9 K (in units at the probe radius) with the expected fall-off.

The resolution for the warm results is about 0.003 through n=8 (0.5 units at 40 mm). These resolutions seem to be at the expected limit from the 16 bit ADC data acquisition. Note that the probe radius was sized to fit the available warm bore tube, which is considerably smaller than the magnet reference radius. Measurements were made at room temperature, 4.5 K, and 1.9 K. During measurements, the magnet was able to remain at 14605A for over an hour without quenching.

IV. Results and Analysis

A. Magnet Geometry, Persistent Current and Iron Saturation Effects

Figures 3 and 4 show the HQ02 harmonics averaged over the axial straight section, and comparison with two HQ01 assemblies and expected requirements. Actual requirements are not yet defined, so those here are based on randomizing conductor position errors achievable during fabrication (30 microns) and calculating the resulting harmonics variation in a vein similar to [7]. The geometric harmonics are fairly well controlled compared to these expected requirements.

The normal and skew sextupole as a function of axial position are shown in Figure 5. The values of b_3 and a_3 show a large systematic effect of several units and changes of the same order. These are likely due to the coil pre-load condition or perhaps to coil azimuthal misalignment inside the collar. This is being studied further.

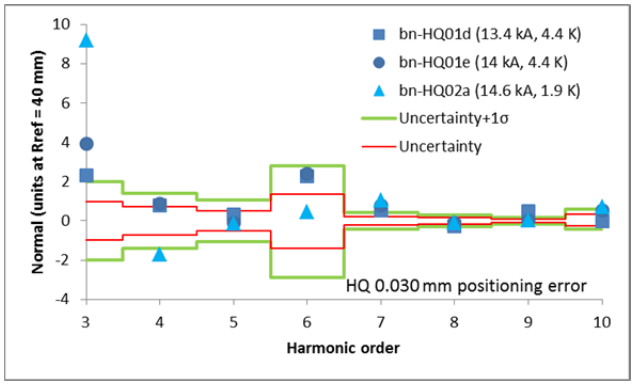

Fig. 3. Normal harmonics at high field compared to expected field quality requirements (as determined from achievable 30 μm fabrication tolerances).

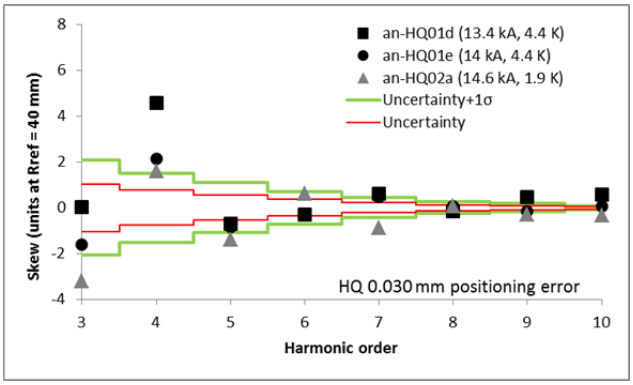

Fig. 4. Skew harmonics at high field compared to expected field quality requirements (as determined from achievable 30 μm fabrication tolerances).

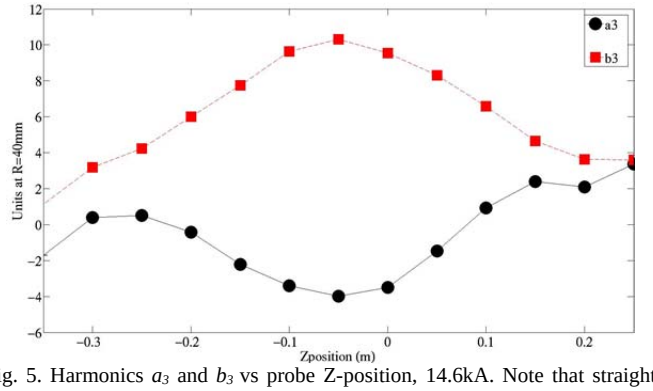

Fig. 5. Harmonics a_3 and b_3 vs probe Z-position, 14.6kA. Note that straight section center, defined by equal values of B_2 in the ends, is Z=-0.05.

The warm/cold correlation of low-order harmonics is shown in Fig. 6. These are generally close (within ~1 unit) to a slope of 1, indicating that it should be possible to detect and compensate such geometrical effects before final assembly.

The persistent current effects, are shown in Figs. 7 and 8 for the quadrupole strength transfer function (TF), and (allowed harmonic) b_6 . The experimental results are in good agreement with OPERA calculations [8] using the cable magnetization data above 2 kA. The effect of iron saturation is also clear in Fig 7, and is measured at about 6% from low to high field. Measurements comparing data taken at 1.9 K and 4.5 K indicate that the dependence on temperature of such effects is small.

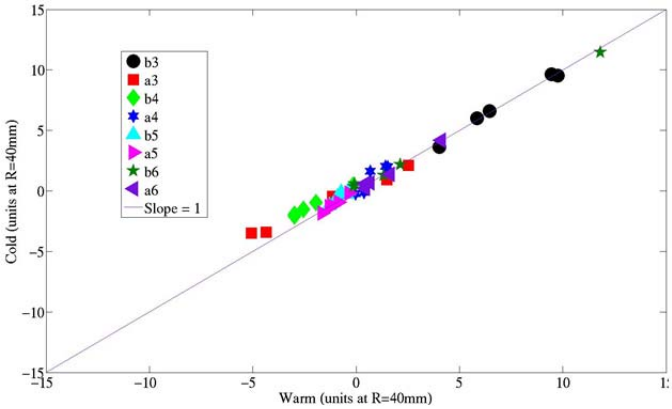

Fig. 6. Harmonics correlation between 1.9 K, 14.6 kA and 300 K, 10 A

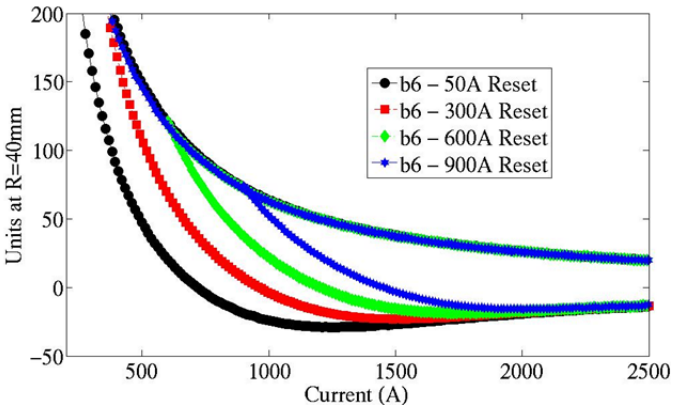

Fig. 9. b_6 during cycles from different minimum currents during accelerator cycles. The value of b_6 at injection can be tuned by choosing the min. current.

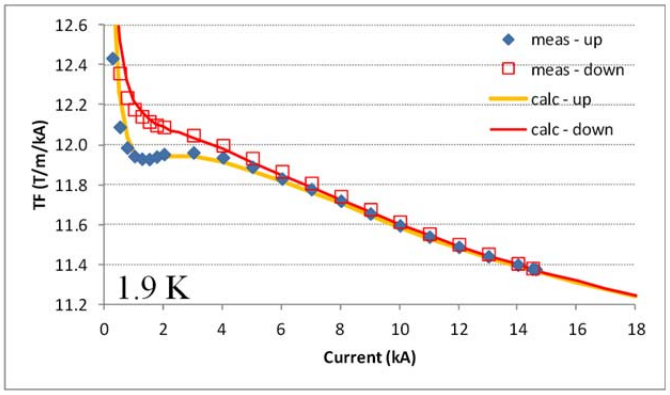

Fig. 7. Persistent current effects in the quadrupole strength transfer function (TF) as a function of current vs calculation from cable data.

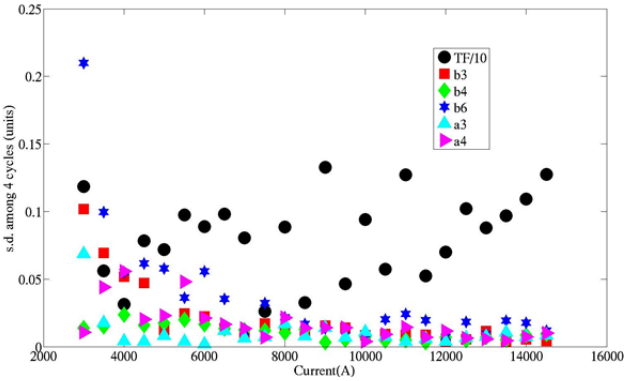

Fig. 10. Standard deviation among 4 cycles at 13 A/s vs. current. Note that the TF has been scaled by a factor 10 for legibility; it has s.d. of ~1 unit.

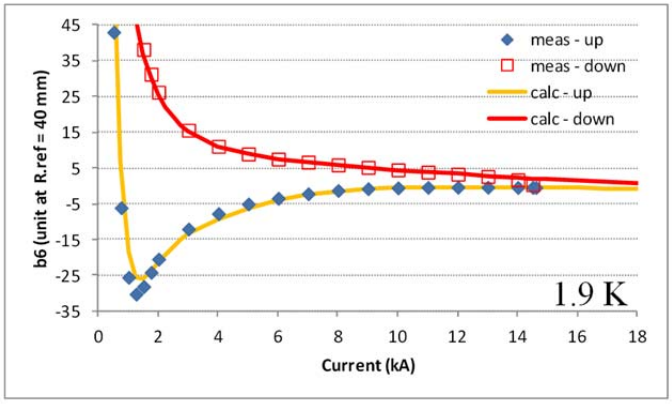

Fig. 8. Persistent current effects in b_6 as a function of current vs calculation from cable data. Note that a shift has been applied to match the geometric component in the data to the calculation.

Measurements varying the minimum (or 'reset') current from which the accelerator cycle begins ramping to injection plateau were performed at 1.9 K. This measures the dependence of the harmonics at injection on the reset current [9], [10]. The trend shown in the results of Fig. 9 indicates the possibility of optimizing the value of b_6 at injection by appropriate choice of minimum current during the cycle.

As a measure of repeatability, Fig. 10 shows standard deviations over four consecutive loop measurements at 13 A/s vs. current. The repeatability of TF is ~1 unit and that of the low order harmonics is typically better than 0.05 units, especially at the higher fields.

B. Eddy Current Effect

To estimate the effect of the eddy currents on the magnet transfer function and the field quality of the single-aperture demonstrator, several excitation loops have been executed at ramp rates of 13 A/s, 20 A/s, 40 A/s, and 80 A/s.

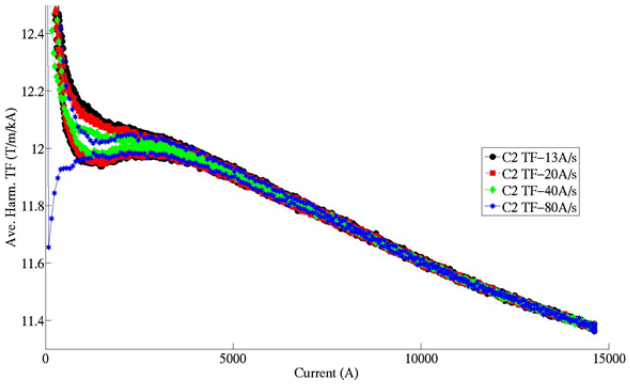

Fig. 11. Transfer function vs. magnet current at var. ramp rates.

Figs. 11 and 12 show the measured variations of the quadrupole transfer function (TF) and b_6 harmonics respectively as a function of the excitation current at different ramp rates. As expected, because of the cored cable, the dependence on ramp rate is small. However, Figs. 13 and 14 show that the corresponding normal sextupole (b_3) and skew sextupole (a_3) field loops show larger ramp rate dependence than the other components, though still about a factor of 10

smaller than seen in HQ01 [2]. The cause of the larger effect observed on the sextupole components is still being investigated. When ramping stops, these effects decay relatively quickly with a time constant of ~4 s.

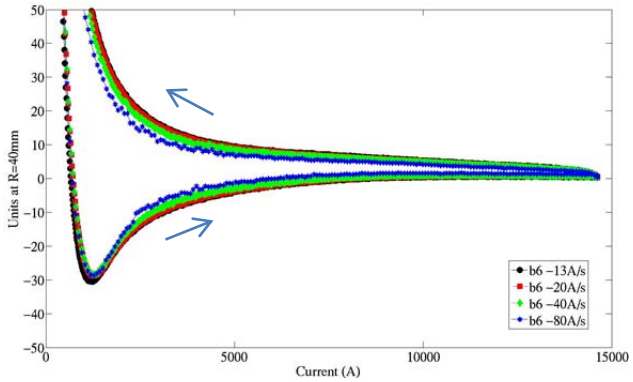

Fig. 12. b_6 vs. magnet current at var. ramp rates.

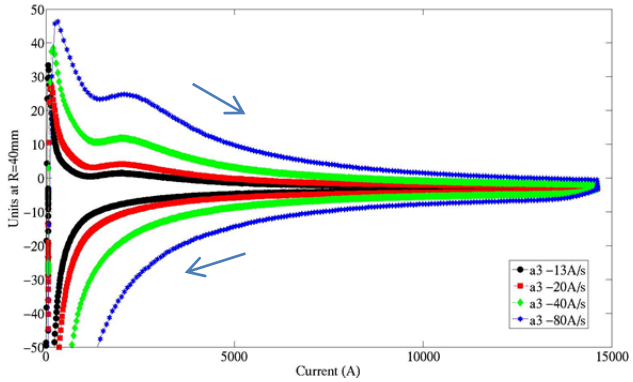

Fig. 13. a_3 vs. magnet current at var. ramp rates.

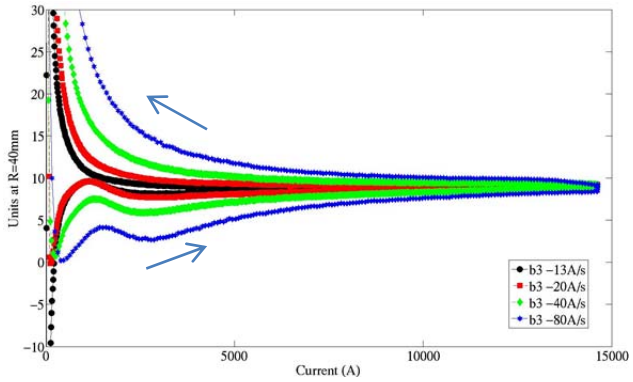

Fig. 14. b_3 vs. magnet current at var. ramp rates .

C. *Long-term Dynamic Effects*

Long-term dynamic effects in superconducting magnets are usually associated with the decay of the allowed field components at injection, which is followed by a subsequent snapback during the acceleration ramp [11], [12].

To investigate these effects in HQ02, measurements with an accelerator current profile similar to one used for the LHC magnets were performed with maximum current of 14.6 kA. The duration of the injection plateau was ~600 s. The decay and snapback in the normal dodecapole component (b_6) is shown in Fig. 15. Decay at injection is small, about 0.5 units.

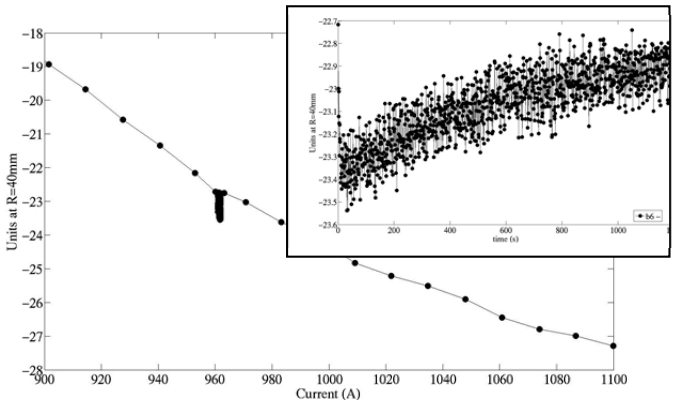

Fig. 15. b_6 in the vicinity of the injection porch (960A) during an accelerator cycle measurement. The inset shows the decay trend of b_6 vs. time at injection.

D. *'Flux-jump' events*

Random disturbances have been observed in the field harmonics during magnet ramping. These are correlated with voltage imbalance effects in the magnet coils and are likely caused by flux redistribution events in the cable. These are being investigated further but seem to have larger amplitude at 4.5 K than at 1.9 K, for example in b_4, as shown in Fig. 16.

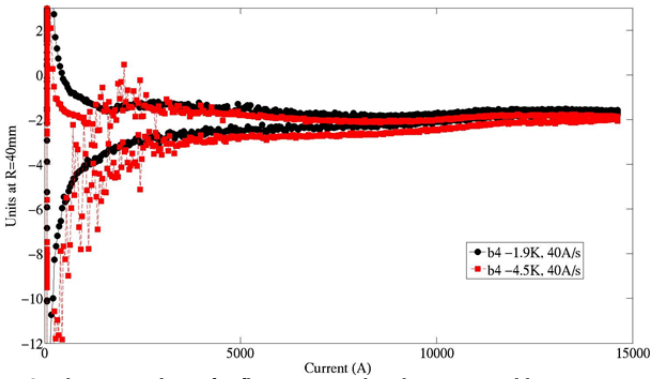

Fig. 16. There is evidence for flux jumps within the magnet cable. Larger amplitude is observed at lower currents and at 4.5 K rather than 1.9 K.

V. Conclusion

Magnetic measurements and analysis were performed for the 1 m long, large-aperture, high-field Nb_3Sn quadrupole HQ02.

The geometrical field harmonics in the magnet body are generally fairly small due to coil cross-section optimization, but low-order terms will need further tuning.

The eddy current effect was successfully removed from the allowed terms with the addition of a stainless steel core in the cable of this magnet. However, there are also relatively large eddy current effects in some low-order non-allowed harmonics (though much smaller than in the previous HQ prototype). These effects continue to be studied.

Acknowledgment

The authors thank M. Sumption and X. Xu at Ohio State University for measuring the strand magnetization (supported by the Office of High Energy Physics, DOE DE-FG02-95ER40900). Also, technical staff of FNAL, BNL, and LBNL for contributions to magnet design, fabrication, and test.

REFERENCES

[1] L. Bottura *et al.*, "Advanced Accelerator Magnets for Upgrading the LHC", *IEEE Trans. Appl. Supercond.*, vol. 22, no. 3, 4002008, 2012.

[2] X. R. Wang, *et al.*, "Multipoles induced by inter-strand coupling currents in LARP Nb_3Sn magnets", *IEEE Trans. Appl. Supercond.* 23 submitted for publication.

[3] F. Borgnolutti, *et al.*, "Fabrication of a second generation of Nb_3Sn coils for the LARP HQ02 quadrupole magnet", *IEEE Trans. Appl. Supercond.* 23 submitted for publication.

[4] A. Jain, "Basic Theory of Magnets", *Proc. CERN Accelerator School*, Anacapri, Italy, CERN-98-05, pp.1-26, 1997.

[5] G.V. Velev *et al.*, "A Fast Continuous Magnetic Field Measurement System Based on Digital Signal Processors", *IEEE Trans. Appl. Supercond.*, vol. 16, no. 2, pp. 1374-1377, June 2006.

[6] J. DiMarco *et al.*, "Application of PCB and FDM Technologies to Magnetic Measurement Probe System Development", *IEEE Trans. Appl. Supercond.*, vol. 23, no. 3, 9000505, 2013.

[7] F. Borgnolutti, *et al.*, "Reproducibility of the Coil Positioning in Magnet Models Through Magnetic Measurements", *IEEE Trans. Appl. Supercond.*, vol. 19, no. 3, pp. 1100-1105, 2009.

[8] X. Wang, *et al.*, "Summary of HQ01e magnetic measurements", LBNL report 5290E, Berkeley, CA, December 2012.

[9] N. Andreev, *et al.*, "Field Quality Measurements in a Single-Aperture 11 T Nb_3Sn Demonstrator Dipole for LHC Upgrades", *IEEE Trans. Appl. Supercond.*, vol. 23, no. 3, 4001804, 2013.

[10] N. Sammut *et al.*, "Mathematical formulation to predict the harmonics of the superconducting large hadron collider magnets: III. precycle ramp rate effects and magnet characterization." *Phys. Rev. Spec. Top. Accel. Beams 12*, 102401, 2009.

[11] G.V. Velev *et al.*, "Measurements of the Persistent Current Decay and Snapback Effect in Tevatron Dipole", *IEEE Trans. Appl. Supercond.*, vol. 17, pp. 1105-1108, 2007.

[12] G.V. Velev *et al.*, "Measurements of the Persistent Current Decay and Snapback Effect in Nb_3Sn Accelerator Prototype Magnets at Fermilab", *Proc. of IPAC2012*, New Orleans, pp. 3593-3595, 2012.